

# Intelligent IMC-PID Control Using PSO for Ultrasonic Motor

Shenglin MU, Graduate School of Engineering, Yamaguchi University, Japan, p002we@yamaguchi-u.ac.jp

Kanya TANAKA, Graduate School of Engineering, Yamaguchi University, Japan, ktanaka@yamaguchi-u.ac.jp

**Abstract:** In this paper, we propose a novel scheme of IMC-PID control combined with a particle swarm optimization (PSO) type neural network (NN) for an ultrasonic motor (USM). In this method, the single control parameter of IMC-PID is adjusted by the NNs. The weights of NNs are updated by PSO algorithm. The proposed method makes it possible to compensate the characteristic changes and nonlinearity of USM. On the other hand, since the PSO algorithm requires no information about USM beforehand, its application overcomes the problem of the Jacobian estimation in the conventional back-propagation (BP) method of NN. The effectiveness of the proposed method is confirmed by experiments using USM servo system.

**Key-Words:** ultrasonic motor (USM), IMC-PID, neural network (NN), particle swarm optimization (PSO).

## 1. Introduction

Ultrasonic motor (USM) is a unique motor which employs frictional force generated by high-frequency mechanical vibration in piezoelectric element as a drive source. It possesses some excellent features, such as lightweight, noiselessness, high torque at low speed range, high retention torque, and no electromagnetic noise. Therefore, USM is considered as an excellent actuator in many industrial fields [1~3].

However, there are still several drawbacks prevent USM from being a precise positioning actuator. Firstly, because of USM's friction drive principle, it is difficult to get mathematical model of USM based on physical analysis. Although some plant models for USM have been proposed, they are too complex to apply modern control theories. Since advanced control theories are hard to be applied on USM, the PID control, which has simple architecture and works well even without mathematical model, has been widely used in USM applications [4-7]. And, the internal model control (IMC)-PID control, which simplifies the tuning of PID gains, has been introduced [8]. Secondly, USM possesses characteristic changes and nonlinearity, which are associated with experimental conditions. Conventional constant gain IMC-PID control cannot solve such problems of USM. Therefore, neural network (NN) has been introduced in recent years [9-12]. However, NN has the problem of local minimum. And, conventional back-propagation (BP) method in NN requires the Jacobian of USM estimated beforehand [13]. In order to solve these problems of NN, we adopt particle swarm optimization (PSO). PSO has been studied in the field of probability optimization in recent years [14-17]. Since PSO is the effective global optimization tool, it can be considered as a good tool to overcome problems of the conventional NN. Therefore, we propose a novel scheme of IMC-PID control combined with a PSO type NN. In the proposed scheme, one parameter of the controller is adjusted by NN to compensate the nonlinearity and characteristic changes of USM. Learning of NN is carried out by PSO instead of the BP method. The effectiveness of the proposed method is validated by experiments using USM servo system.

This paper is organized as the follows. The conventional

IMC-PID is introduced in Sec. 2. The NN and PSO algorithms applied in the paper are presented in Sec. 3. Section 4 introduces the USM servo system and experimental setup. The experimental results and discussions are given in Sec. 5. Section 6 presents the conclusions in the end.

## 2. Conventional IMC-PID Control

### 2.1 PID Control

The PID control is the most widely used control scheme in industrial fields. Figure 1 shows the scheme of PID control considered in this paper. In the scheme,  $r(k)$ ,  $u(k)$ , and  $y(k)$  are the object input, the input and the output, respectively.  $G_{PID}(z^{-1})$  is the PID controller. The input  $u(k)$  is synthesized as

$$u(k) = u(k-1) + (K_P + K_I + K_D)e(k) - (K_P + 2K_D)e(k-1) + K_D e(k-2) \quad (1)$$

where  $K_P$ ,  $K_I$  and  $K_D$  are the gains of the PID controller. The error denoted by  $e(k)$  expressed as

$$e(k) = r(k) - y(k) \quad (2)$$

Furthermore, the PID controller  $G_{PID}(z^{-1})$  can be denoted as Eq. (3) shows.

$$G_{PID}(z^{-1}) = \frac{K_P(1 - z^{-1}) + K_I + K_D(1 - z^{-1})^2}{1 - z^{-1}} \quad (3)$$

### 2.2 IMC-PID Control

The IMC-PID control requires a mathematical model of the plant. However, the mathematical model of USM is very difficult to derive. Here we adopt a virtual plant model of USM

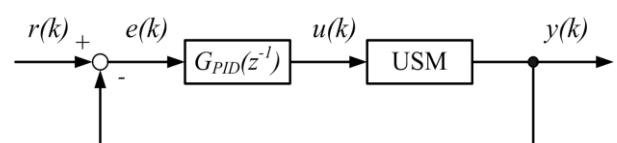


Figure 1 Block diagram of PID control

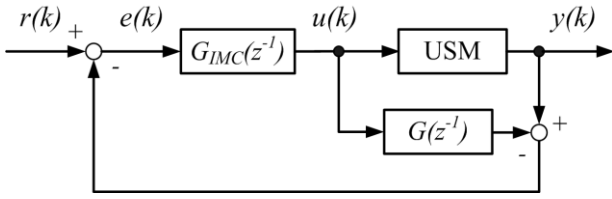


Figure 2 Block diagram of IMC control

expressed as

$$y(k) = G(z^{-1})u(k) \quad (4)$$

where

$$G(z^{-1}) = \frac{b_0 z^{-1}}{A(z^{-1})} \quad (5)$$

and

$$A(z^{-1}) = 1 + a_1 z^{-1} + a_2 z^{-2} \quad (6)$$

Figure 2 shows the block diagram of the IMC scheme.  $G_{IMC}(z^{-1})$  means the IMC controller.  $G(z^{-1})$  connected to the USM in parallel is the internal model expressed as the same form in Eq.(5).  $G(z^{-1})$  can be divided into a minimum phase element  $G_M(z^{-1})$  and a lag time  $z^{-1}$  [8,18,19] expressed as

$$G(z^{-1}) = G_M(z^{-1}) \cdot z^{-1} \quad (7)$$

where

$$G_M(z^{-1}) = \frac{b_0}{A(z^{-1})} \quad (8)$$

We define a first-order lag filter as the following shows.

$$f(z^{-1}) = \frac{1-\alpha}{1-\alpha z^{-1}} \quad (9)$$

where  $\alpha$  is a control parameter which can be decided arbitrary within the range of  $0 \leq \alpha < 1$ . The controller  $G_{IMC}(z^{-1})$  can be expressed as

$$\begin{aligned} G_{IMC}(z^{-1}) &= G_M^{-1}(z^{-1}) \cdot f(z^{-1}) \\ &= \frac{1 + a_1 z^{-1} + a_2 z^{-2}}{b_0} \cdot \frac{1-\alpha}{1-\alpha z^{-1}} \end{aligned} \quad (10)$$

The IMC scheme can be expressed as a feedback control structure as Fig.3 shows. The controller  $G_C(z^{-1})$  can be expressed by Eq.(11).

$$G_C(z^{-1}) = \frac{\bar{K}_p(1-z^{-1}) + \bar{K}_I + \bar{K}_D(1-z^{-1})^2}{1-z^{-1}} \quad (11)$$

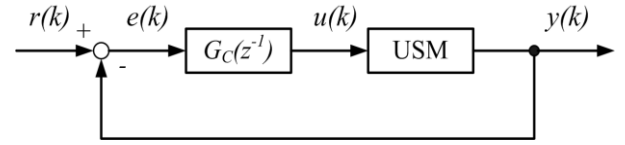


Figure 3 Block diagram of feedback controller

where

$$\begin{aligned} \bar{K}_p &= -(1-\alpha) \cdot \frac{a_1 + 2a_2}{b_0} \\ \bar{K}_I &= (1-\alpha) \cdot \frac{1+a_1+a_2}{b_0} \\ \bar{K}_D &= (1-\alpha) \cdot \frac{a_2}{b_0} \end{aligned} \quad (12)$$

Using above gains, the control input can be synthesized as

$$\begin{aligned} u(k) &= u(k-1) + (\bar{K}_p + \bar{K}_I + \bar{K}_D)e(k) \\ &\quad - (\bar{K}_p + 2\bar{K}_D)e(k-1) + \bar{K}_D e(k-2) \end{aligned} \quad (13)$$

### 3. PSO Type Neural Network

Since the conventional fixed gain type IMC-PID controller stated above is difficult to compensate nonlinearity and characteristic changes of USM. On the other hand, NN is the effective tool to overcome these problems. However, the conventional NN contains of the local minimum and the Jacobian problem. To overcome all problems, we would like to propose the novel design scheme of IMC-PID combined with the PSO type NN. Figure 4 shows the proposed design scheme. In Fig.4, the system parameter  $\alpha(k)$  is the output from the PSO type NN(PSO-NN). Weights of NN are tuned by PSO to compensate the nonlinearity and characteristic changes of USM.

#### 3.1 Neural Network

In this application, an NN controller with a two-layer structure is applied. The structure of the NN controller is shown in Fig.5. Four neurons are set in the input layer.  $I_i(k)$  expressed in Eq.(14) is the input of NN.

$$I_i(k) = \{y(k), y(k-1), y(k-2), u(k-1)\} \quad (14)$$

As Fig.5 shows,  $\alpha(k)$  is designed as the output of the NN and used as the control parameter in the IMC-PID controller. It can

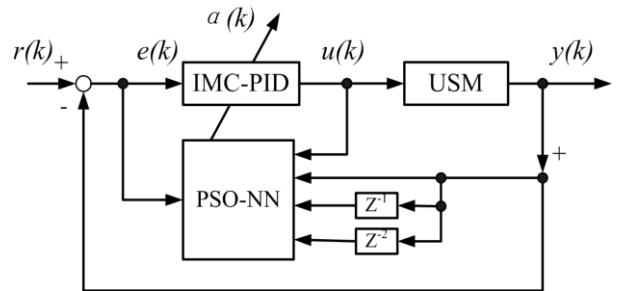


Figure 4 Block diagram of the proposed scheme

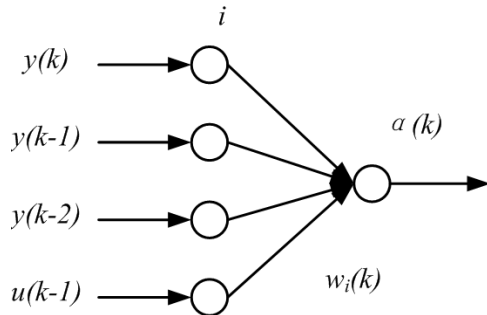


Figure 5 Structure of neural network

be expressed as

$$\alpha(k) = f_s(\text{net}_i) \tag{15}$$

where the function  $f_s(k)$  means the sigmoid function as Eq.(16) shows.

$$f_s(x) = \frac{1}{1 + e^{-x}} \tag{16}$$

The  $\text{net}_i$  can be calculated as

$$\text{net}_i = \sum_i^4 w_i(k)I_i(k) \tag{17}$$

where  $w_i(k)$  presents the weights in the connections. They are designed to be updated by the PSO algorithm in this scheme.

### 3.2 Particle Swarm Optimization

PSO is a global optimization algorithm discovered through the simulation of a simplified social model. Since it is simple in concept and easy to implement, it is quite attractive in the field of probability optimization in recent years [14-16].

Figure 6 shows an example of particle movement of PSO.  $x_i(k)$  means the position of the  $i_{th}$  particle in the  $k$  step,  $x_i(k-1)$  and  $x_i(k+1)$  mean the position of the  $(k-1)$  step and the  $(k+1)$  step, respectively.  $gbest$  is the best position of the whole swarm, and  $pbest$  is the best position of the particle.  $v_i(k)$ , which expresses the position variance, is the velocity of the particle at the  $k$  step. It is related to the best positions as the dash lines show in the figure.

In NN learning, we define the value of weights as the position information contained by N particles. The position of the  $n$ th particle is defined as  $X_n=[w1, w2, w3, w4]$ . And, the velocity can be expressed as  $V_n=[v1, v2, v3, v4]$ . The weights are designed to be updated by an inertia weight approach

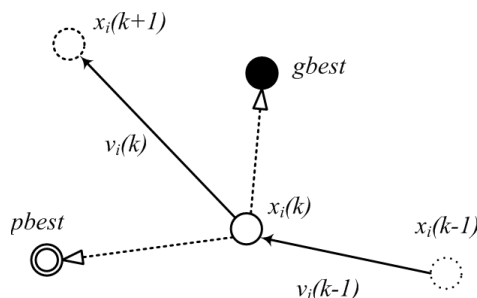


Figure 6 Example of particle movement of PSO

(IWA) type PSO algorithm expressed in Eq.(18) and Eq.(19).

$$V_{n+1} = \tau \cdot V_n + c_1 \cdot r_1 \cdot (pbest_n - X_n) + c_2 \cdot r_2 \cdot (gbest_n - X_n) \tag{18}$$

$$X_{n+1} = X_n + V_n \tag{19}$$

In Eq.(18),  $c_1$  and  $c_2$  are two positive constants,  $r_1$  and  $r_2$  are two random numbers within [0,1]. In Eq.(19), the weight factor which balances the global and local search, is calculated as Eq.(20) shows.

$$\tau = \tau_{\max} - \frac{\tau_{\max} - \tau_{\min}}{episode_{\max}} \cdot episode \tag{20}$$

where  $episode$  means the number of current iteration,  $episode_{\max}$  presents the max iteration number in the searching.  $\tau_{\max}$  and  $\tau_{\min}$  are the weight factor's maximum and minimum value, respectively. The specification of the PSO type NN algorithm for experiment is to be introduced in Section 5.

## 4. USM Servo System

In this section, the USM servo system is presented. Figure 7 shows the structure of the system. The USM, the encoder, and the magnetic brake are connected on a common axis. The position signal fetched by the encoder is input to the counter board connected to the PC. Information of the control input calculated from the output and the object input in the PC is transferred to the driving circuit via the I/O board.

Table 1 shows the specifications of the USM, the encoder and the load. Table 2 shows the specifications of the driving circuit. The driving circuit is shown in Fig.8. The phase difference control circuit is constructed by a digital circuit with a shift register. The voltage control and the voltage control circuit at the final stage are constructed by a digital potential meter, a digital operational amplifier, and a booster transistor. To make stable start, a driving frequency is fixed at 36.0 kHz

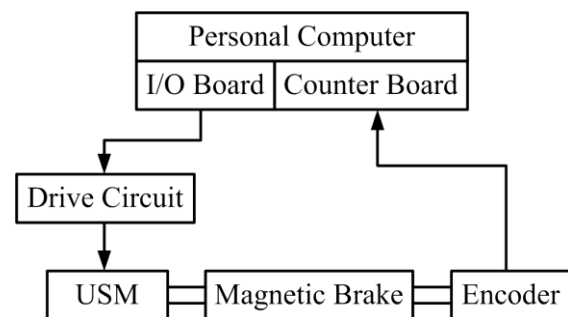


Figure 7 USM servo system

Table 1 Specifications of USM, encoder and load

USM	Rated rotational speed: 100 rpm
	Rated torque: 0.392 N·m
	Holding torque: 0.392 N·m
Encoder	Resolution: 0.0036 deg.
Load	0~0.2 N·m

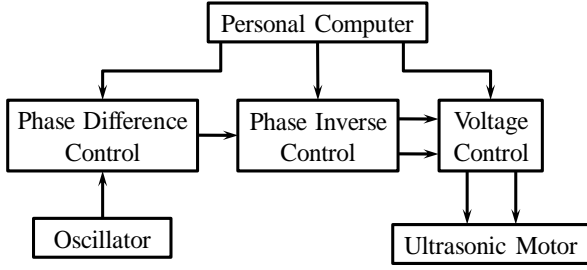


Figure 8 Drive circuit of USM servo system

Table 2 Specifications of the drive circuit

Driving frequency	36.0 kHz
Driving voltage	150 V
Phase difference	-90~90 deg.
Resolution of phase difference	1.406 deg.
Sampling time	1.0 ms

which is 1.0 kHz higher than resonance frequency of the USM. For the USM driving, the phase difference control method adopted. The method prevents hysteresis phenomenon and has a relatively linear relation between input and output. The phase difference is adjusted between -90 deg. and 90 deg. by 1.406 deg.

## 5. Experiments and Results

### 5.1 Experimental Setups

In order to confirm the effectiveness of the proposed method, a group of experiments are implemented in the USM servo system. The purpose of the experiments is to validate the performance of this proposed method in reducing the steady-state error in the precise position control.

The object input  $r(k)$  is a rectangular signal. The amplitude is set from +45 deg. to -45 deg. The period is 6 sec. In this paper, we call the position, expressed by +45 deg., as clockwise rotation. The opposite one, expressed by -45 deg., is the counter-clockwise rotation. For comparison, a group of conventional IMC-PID experiments are implemented. We set a group of optimized system identification parameters for the conventional IMC-PID control. The value parameters are set as  $a_1=-0.4966$ ,  $a_2=-0.4894$ ,  $b_0=0.03$ , and  $\alpha$  is set as 0.6.

Due to different characteristics of clockwise and counter-clockwise turning, in the proposed method, two independent NNs are assigned to the clockwise and counter-clockwise rotations. Two swarms with 10 particles respectively are designed for the NNs. All the particles are initialized by random numbers from -1 to 1. Learning of NN, which is the executed by PSO, is carried from 1.0 sec. to 1.5 sec. after changing the sign of the object input. The parameter episode in Eq.(20) varies from 1 to 50, and  $episode_{max}$  is 50. The inertia weight factors  $\tau_{max}$  and  $\tau_{min}$  are set as  $\tau_{max}=0.9$  and  $\tau_{min}=0.4$ , respectively. The positive constants  $c_1$  and  $c_2$  are set as  $c_1=c_2=2.0$ . The particles are designed to be evaluated by the following function fitness, ( $f \in [0,1]$ ), using the real-time error  $e(k)=r(k)-y(k)$ .

The fitness is updated by each millisecond. Since the precise resolution of encoder makes the fitness variation insensitive, we enlarge  $e(k)$  by 100 times to make  $fitness$  response quickly

in the experiments.

$$fitness = \frac{1}{(1+100 \cdot e(k))^2} \quad (21)$$

### 5.2 Results and Study

In the experiments, the rectangular wave signal is set to run 30 cycles. Figure 9 shows the response of the last two cycles in the experiment. We can see that the output follows the object input almost in a steady state. Figure 10 shows the variation of  $\alpha(k)$ , the NN output in the first 5 cycles. We can see that after about 3 cycles learning, the outputs of clockwise and counter-clockwise NN converged to different value. It can be stated that the USM has the different characteristic according to the rotatory direction, and that the proposed method is capable to search optimal value for each rotatory direction. Figure 11 and 12 show the weights updating of NN, respectively. The weights of the clockwise and the counter-clockwise converged to different values within 5 cycles. It can be concluded that PSO is an effective tool to adjust weights of NN. For comparison, positioning errors of conventional method and proposed method in the steady state have been evaluated. The errors were sampled at each 0.1 second before direction changing. Figure 13 shows the histogram of the positioning error with no load of the conventional IMC-PID method. We can see that errors are from -0.0072 to 0.0036 deg. in clockwise rotation and are from -0.0288 to 0.0144 deg. in counter-clockwise rotation. It can be concluded that the

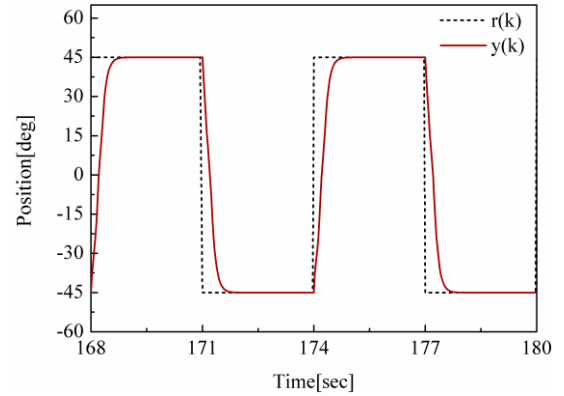
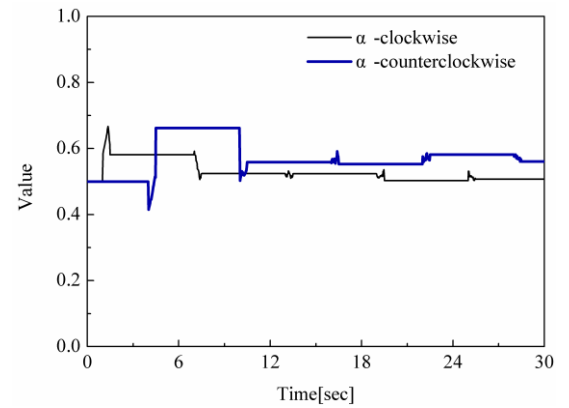


Figure 9 Response of the proposed method


 Figure 10 Variation of the control parameter  $\alpha(k)$

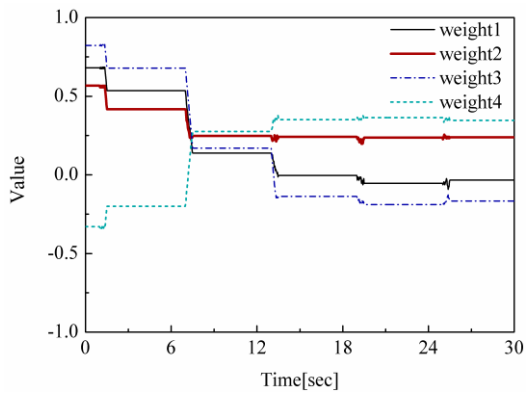


Figure 11 Weights of the clockwise turning.

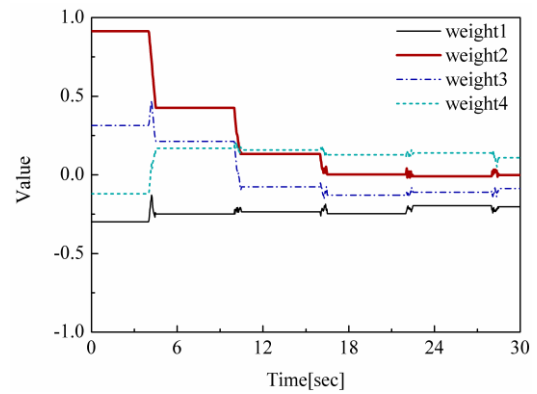


Figure 12 Weights of the counter-clockwise turning.

identification parameters of conventional IMC-PID are good at describing the characteristic of the USM. And the clockwise performance is better than the counter-clockwise performance. Figure 14 shows the histogram of the positioning error with no load of the proposed method. Errors distribute from -0.0036 to 0.0036 deg. in clockwise rotation and from -0.0036 to 0.0072 deg. in counter-clockwise rotation. From the results, we can see that the control performance of the proposed method is superior to ones of the conventional method.

Figure 15 shows the histogram of the positioning error with

the load (0.05 N·m) of the conventional IMC-PID control. Errors distribute from -0.0108 to 0 deg. in clockwise rotation and from 0.0144 to 0.0216 deg. in counter-clockwise rotation. It proves that the conventional IMC-PID control cannot compensate the nonlinearity and characteristic changes when the load is added to USM. Then, we can see the positioning errors of the proposed method shown in Fig. 16 shows the histogram of the positioning error with the load (0.05 N·m) of the proposed method. Errors concentrate on -0.0036 deg. in clockwise rotation and distribute from 0 to 0.0036 deg. in

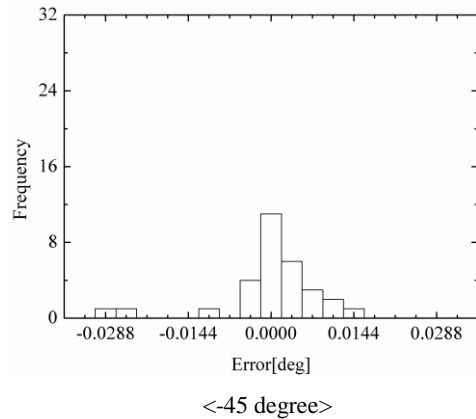
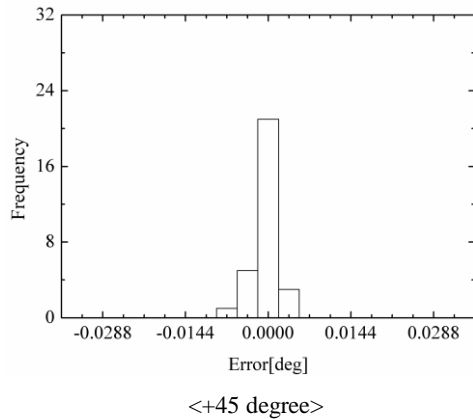


Figure 13 Positioning error of the conventional IMC-PID (no load).

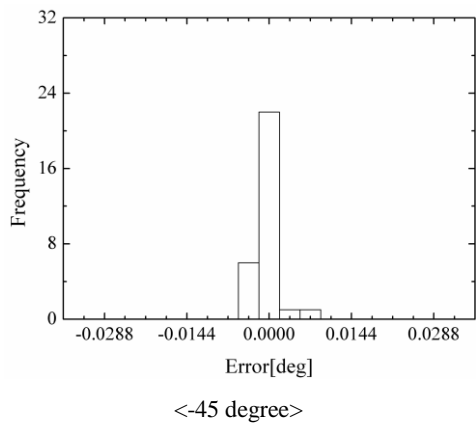
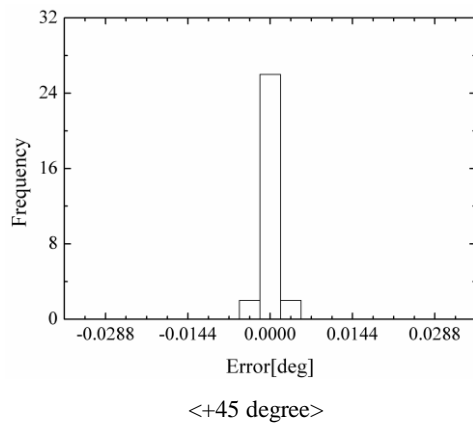


Figure 14 Positioning error of the proposed method (no load).

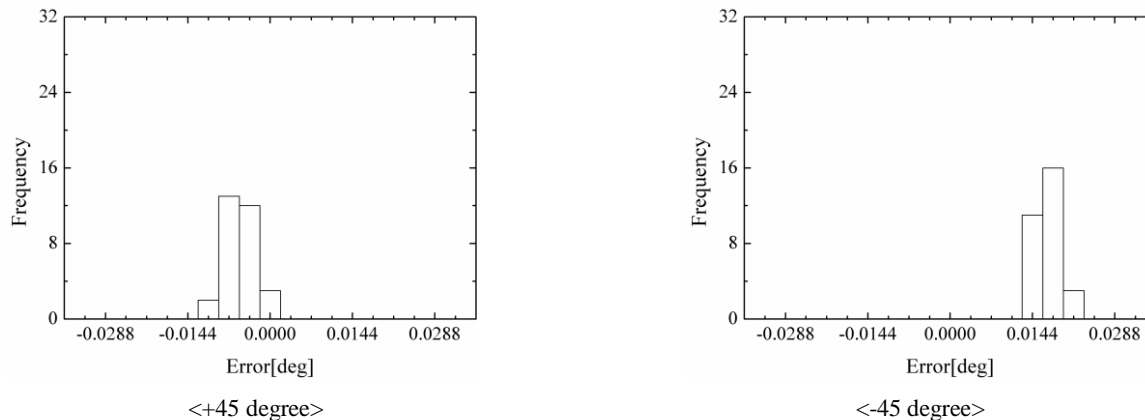


Figure 15 Positioning error of the conventional IMC-PID (load: 0.05 N·m).

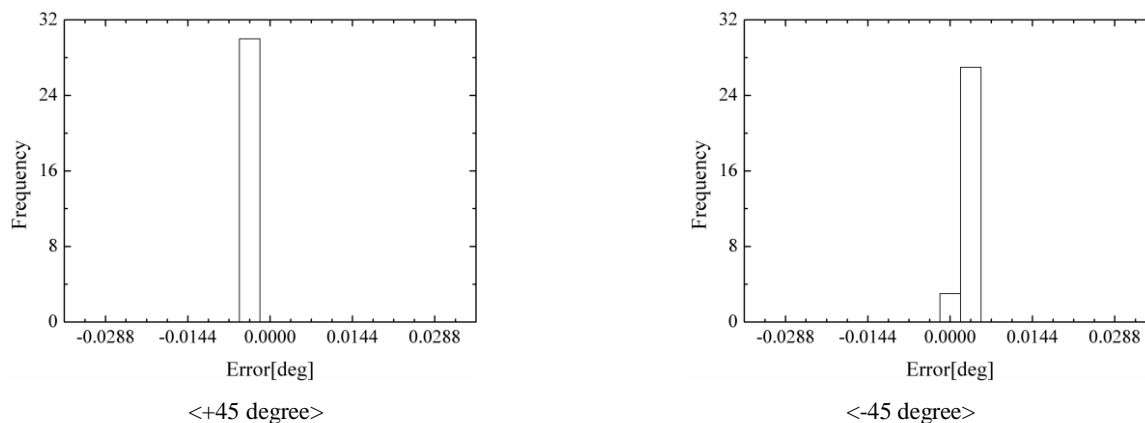


Figure 16 Positioning error of the proposed method (load: 0.05 N·m).

counter-clockwise rotation. We can see that the positioning error of the proposed method is improved than ones of the conventional method obviously. From these experimental results, the effectiveness of the IMC-PID control with PSO-NN has been confirmed.

## 6. Conclusions

In this paper, a novel IMC-PID control scheme combined with PSO type NN has been proposed for precise positioning control of USM. The NN is used for optimizing the control parameter of the IMC-PID controller and the PSO algorithm is applied in NN's learning. The proposed method overcomes the Jacobian estimate problem of conventional BP type NN. The proposed method can compensate not only the characteristic changes but also nonlinearity of USM. The effectiveness of the proposed method is confirmed by experiments using USM servo system.

## References:

- [1] T. Kenjyo and T. Sashida: "An Introduction of Ultrasonic Motor", Oxford Science Publications, 1993.
- [2] T. Maeno, T. Tsukimoto and A. Miyake: "Finite-Element Analysis of the Rotor/Stator Contact in a Ring-Type Ultrasonic Motor", IEEE Trans. Ultrasonics, Ferroelectrics, and Frequency Control, Vol.39, No.6, 1992, pp.668-674.
- [3] T. Maeno: "Ultrasonic Motor", JRSJ, Vol.21, No.1, 2003, pp.10-14.
- [4] J.G.Ziegler and N. B. Nichols: "Optimum Settings for Automatic Controllers", Trans. ASME, Vol.64, 1942, pp.759-768.
- [5] P. Hazebroek and B. L. van der Waerden: "The Optimal Adjustment of Regulators", Trans. AMSE, No.72, 1950, pp.312-322.
- [6] W. A. Wolfe: "Controller Settings for Optimum Control", 1951, Trans. ASME, No.73, pp.413-418.
- [7] C. E. Garcia and M. Morari: "Internal Model Control-1. A Unifying Review and Some New Results", Ind. Eng. Process Des. & Dev.21, 1982, pp.318-323.
- [8] J. Li and K. Tanaka: "Intelligent control for Pneumatic Servo System", JSME International Journal, Series C, Vol.46, No.2, 2003, pp.699-704.
- [9] K. Tanaka, M. Oka, A. Uchibori, Y. Iwata and H. Morioka: "Precise Position Control of Ultrasonic Motor Using PID Controller Combined with NN", IEEJ Journal, Series C, Vol.122, No.8, 2002, pp.1317-1324.
- [10] K. Tanaka, T. Takeguchi, J. Nakamoto, and Jinhua Li: "IMC-PID Control Using NN for Ultrasonic Motor", IEEJ Trans. EIS, Vol.123, No.11, 2003, pp.1982-1988.
- [11] M. Oka, K. Tanaka, A. Naganawa and K. Haruyama: "Precise Position Control of the Ultrasonic Motor Using Input-Output Linear Compensation Type Controller", Journal of AEM, Vol.15, No.2, 2007, pp.149-155.
- [12] K. Fukuda, T. Kamano, T. Suzuki, T. Yasuno and H. Harada: "High accuracy positioning system with ultrasonic motor using frequency and phase neural networks", Journal of AEM, Vol.6, No.4, 1998, pp.44-51.
- [13] K. Tanaka, M. Oka, Y. Wakasa, T. Akashi, and A. Naganawa: "GA Adjustment Type NN-PID Control for Ultrasonic Motor", Journal of AEM, Vol.15, No.4, 2007, pp.55-61.
- [14] J. Kennedy and R. Eberhart: "Particle Swarm

- Optimization”, Proc. IEEE Int. Conf. Neural Networks, Perth, Australia, 1995, pp.1942-1948.
- [15]M. Clerc and J. Kennedy: “The Particle Swarm: Explosion, Stability, and Convergence in a Multi-Dimensional Complex Space”, IEEE Trans. Evolutionary Computation, Vol.6, No.1, 2002, pp.58-73.
- [16]J. Kennedy, R.C. Eberhart, “Swarm Intelligence”, Morgan Kaufmann Publishers, 2001.
- [17]M. Ito and M. Tanaka: “A Study of Particle Swarm Optimization for Neural Network Training”, A publication of Electronics, Information and System Society, 2005, pp.1087-1089.
- [18]K. Tanaka, Y. Yoshimura, Y. Wakasa, T. Akashi: “Variable Gain Type Internal Model Control-PID Speed Control for Ultrasonic Motor”, IEEJ Trans. IA, Vol.128, No.12, 2008, pp.1326-1332.
- [19]K. Tanaka, Y. Yoshimura, Y. Wakasa, T. Akashi, M. Oka, S. Mu: “Variable Gain Type Intelligent PID Control for Ultrasonic Motor”, Journal of AEM, Vol.17, No.3, 2009, pp.107-113.

